

Enclosure 2

WCAP-7964, “Axial Xenon Transient Tests at the Rochester Gas and Electric Reactor”

(Non-Proprietary)

**Westinghouse Electric Company
1000 Westinghouse Drive
Cranberry Township, PA 16066**

**© 2022 Westinghouse Electric Company LLC
All Rights Reserved**

WCAP-7964

AXIAL XENON TRANSIENT TESTS AT THE
ROCHESTER GAS AND ELECTRIC REACTOR

J. C. Lee
K. A. Jones
D. P. Felentzer
D. Rawle

June, 1971

APPROVED: *A. F. McFarlane*
A. F. McFarlane, Manager
N. E. Branch I, Nuclear Fuel Division

APPROVED: *F. L. Langford*
F. L. Langford, Manager
Nuclear Operations, PWR Systems Division

Work Performed under S.O. DGRP-43001, DGRP-04001, and DGRP-05002

Westinghouse Electric Corporation
Nuclear Energy Systems
P. O. Box 355
Pittsburgh, Pennsylvania 15230

INADMISSABLE AS EVIDENCE PURSUANT TO
THE AGREEMENT OF WOG DESIGN DOCUMENT
SUBGROUP MEMBER AND WESTINGHOUSE

TABLE OF CONTENTS

Section	Page
LIST OF TABLES	ii
LIST OF FIGURES	iii
ABSTRACT	iv
1. INTRODUCTION	1
2. DESCRIPTION OF THE TESTS	3
2.1 First Test at a Burnup of 1550 MWD/T	3
2.1.1 Phase I - Uncontrolled Oscillation	4
2.1.2 Phase II - Controlled Oscillation	4
2.1.3 Experimental Data	7
2.2 Second Test at a Burnup of 7700 MWD/T	9
3. STABILITY INDEX FROM THE EXPERIMENTAL DATA	23
3.1 The Concept of the Stability Index	23
3.2 Results of the First Test	24
3.3 Results of the Second Test	24
4. ANALYSIS OF THE TESTS	27
4.1 Calculational Model	27
4.2 Results of Calculation	28
4.2.1 Core Stability Calculation	28
4.2.2 Direct Simulation of the Tests	32
5. CONCLUSIONS	35
ACKNOWLEDGEMENTS	37
REFERENCES	38

LIST OF TABLES

Table		Page
1	Stability Index and Period for the First RGE Test	25
2	Comparison of the Two RGE Tests	25
3	RGE Stability Index Calculation	29

<u>LIST OF FIGURES</u>		Page
Figure		
1	Axial Offset Vs. Time, Phase I, First Test	8
2	Detector Current from Channel 41A, Phase I, First Test	10
3	Detector Current from Channel 42A, Phase I, First Test	11
4	Detector Current from Channel 43A, Phase I, First Test	12
5	Detector Current from Channel 44A, Phase I, First Test	13
6	Detector Current from Channel 45A, Phase I, First Test	14
7	Detector Current from Channel 46A, Phase I, First Test	15
8	Power, Bank D, P/L and Axial Offset Vs. Time, Phase II, First Test	16
9	Bank D and Axial Offset Vs. Time during Perturbation, Second Test	18
10	Axial Offset Vs. Time, Second Test	19
11	Axial Offset Data from Channel NE42, Second Test	20
12	Axial Offset Vs. Time	21
13	Average Axial Power Distribution	22
14	Axial Offset Vs. Time, Phase I, First Test	33
15	Axial Offset Vs. Time, Phase II, First Test	34

ABSTRACT

As part of a program to demonstrate that power redistribution transients can be monitored and controlled, two axial xenon tests were conducted at the Rochester Gas and Electric reactor.

The first test, conducted at a core average burnup of 1550 MWD/T, showed that the core was stable against axial xenon transients with a stability index of -0.041 hr^{-1} . The effectiveness of the part length control rods in shaping the axial power distributions was also demonstrated.

The second test was conducted at a core average burnup of 7700 MWD/T. A stability index of -0.014 hr^{-1} was measured showing that the core became less stable due to fuel depletion.

Calculations of the stability indices and the direct simulation of the tests show a reasonable agreement with the measurements, with a conservative margin of 0.01 hr^{-1} in the stability indices.

SECTION 1

INTRODUCTION

The first measurements of core stability against xenon-induced spatial oscillations in a commercial power plant were made at the Connecticut Yankee (CYW) Reactor^[1] in 1969. The CYW tests showed that the PWR with a ten-foot core height and stainless steel clad fuel pellets was stable against axial xenon transients. A stability index of -0.20 hr^{-1} was measured in a pseudo-random test and -0.049 hr^{-1} in an impulse test. (The concept of the stability index is explained in Section 3.1.) These tests also established the adequacy of the experimental techniques used in measuring core stability.

As part of a continuing program to demonstrate that power redistribution transients in a PWR can be monitored and controlled, a series of two axial xenon oscillation tests were performed at the Rochester Gas and Electric (RGE) reactor. The RGE reactor is a PWR with a core height of 12 feet and zircaloy clad fuel pellets. The first test in RGE was conducted in May, 1970 at a core average burnup of 1550 MWD/T and the second in February, 1971 at a core average burnup of 7700 MWD/T, respectively. The objectives of the tests were:

1. To demonstrate that the RGE plant is stable against axial xenon transients early in life.
2. To demonstrate that the axial xenon oscillations can be effectively dampened and controlled by utilization of the part length control rods.

3. To verify that the fuel depletion effects do not compromise the ability to monitor core power distribution parameters with the excore nuclear detectors.
4. To determine the stability of the depleted core against induced axial xenon transients.
5. To provide experimental data for comparison with calculations.

This report describes both the experiment and the analysis of the two RGE tests. Section 2 contains the description of the tests, followed by the actual experimental data. A brief description of the concept of the stability index is presented in Section 3, together with the results of the reduced experimental data. In Section 4 the method and the results of the simulation and analysis of the tests are presented. Conclusions and recommendations follow in Section 5.

SECTION 2

DESCRIPTION OF THE TESTS

It was demonstrated in the tests conducted at CYW^[1] that a perturbation to equilibrium power and xenon distribution in the form of an impulse motion of control rods was adequate for measurement of the core stability against induced axial xenon transients. The same experimental technique was used in both of the RGE tests for measurement of the stability indices of the core. The total core power was maintained constant during these spatial xenon tests in order to measure the stability of the first flux overtone. A trial was also made in the first test to verify the effectiveness of the part length (PL) control rods in controlling an axial xenon transient.

2.1 First Test at a Burnup of 1550 MWD/T

This test consisted of two phases. In Phase I, the uncontrolled part, an axial xenon transient was initiated in the core by inserting Control Group D approximately 30% into the core for a period of four hours. Control Group D was then withdrawn and the resulting xenon oscillations were monitored until the transient had decayed and the axial power distribution was stabilized.

In Phase II the xenon transient was initiated as a result of a natural plant transient, although it was planned originally to initiate the transient using the procedure followed in Phase I. Phase II was the controlled portion of the test and the part length rods were used to follow the oscillations to maintain an axial offset within prescribed limits.

During the entire test, power was maintained at a constant level of approximately 85% of full power. Part length rods remained fixed at mid-plane except for the period when they were used for

dampening. Control Group D was in the manual control mode and remained fixed except during the time when the xenon perturbation was initiated and during the time when the part length rods were used to dampen the xenon oscillation. The reactor was controlled by varying boron concentration, T_{avg} , and turbine load.

Throughout the test incore flux maps were obtained at selected times. Hourly data were recorded for various plant parameters among which were excore detector data and calorimetric data.

2.1.1 Phase I - Uncontrolled Oscillation

Starting from an equilibrium condition with Control Group D at 207 steps and the part length rods at 85 steps, the xenon perturbation was initiated by moving Control Group D to 165 steps for a period of four hours. After the four hour period, Control Group D was withdrawn to its reference position of 207 steps where it remained for the duration of the Phase I testing. The part length rods remained at mid-core (85 steps) for the duration of the Phase I test. The ensuing xenon transient was monitored via the incore instrumentation system and the excore detectors. In addition, calorimetric data were obtained periodically in order to correct for power variations during the test. The test lasted 65 hours and was terminated due to a reduction in load. The original attempt for the Phase I test was aborted halfway due to another load reduction.

2.1.2 Phase II - Controlled Oscillation

Originally the spatial xenon oscillations for this test were to be initiated as they were in Phase I. However, due to the unplanned load reduction at the end of Phase I, a severe xenon transient had already been initiated. The transient was initiated as the result of an unanticipated turbine load runback. This transient was representative of the type of transient which could occur under practical conditions.

The exact character of the transient was not known as would be the case after an unanticipated load reduction and return to power. Therefore, controlling this transient with part length rods was certainly a good test of the effectiveness of the part length rods and of the strategy for their use. In light of these considerations it was felt that this transient would be ideal for the Phase II test. Therefore, the decision was made to start the Phase II testing immediately upon the termination of Phase I.

Phase I ended with Control Group D moving from its equilibrium position of 207 steps to approximately 70 steps. The part length rods remained fixed at mid-core (85 steps). Power dropped from 85% to approximately 58%. Xenon began to increase in the top of the core. At this point, the xenon transient for Phase II was initiated.

Before using the part length control rods to shape the axial power profile, two adjustments had to be made.

1. The part length rods had to be removed from the core. It was felt that by starting with the part length rods in the most adverse position a more severe and consequently a more demonstrative test would be performed.
2. The power had to be raised from 58% of full power to the reference level of 85% full power.

First, the part length rods were borated out of the core. At the same time Control Group D was moved to 165 steps, in order to insure that the axial xenon transient would be large and make the test more severe.

Approximately 10 minutes after the part length rods were withdrawn, the power escalation to 85% of full power began. Power escalation took approximately 50 minutes and was accomplished by withdrawing Control Group D and reducing the boron concentration in the primary coolant. By

the time this was completed, xenon had started to burn out in the top of the core. With the removal of poison in the top of the core, power began to increase. Power also began to increase due to the initial decrease of xenon after the power increase. To prevent the power from increasing, Control Group D automatically began moving into the core, increasing the relative power in the bottom of the core. Consequently, the axial offset was very rapidly becoming more negative. Within approximately 45 minutes after the reference power level had been attained, Control Group D had moved from its starting position of 193 steps to 160 steps and the axial offset (A.O.) of power had changed from -9% to -15%. (Here the A.O. of power is defined as the normalized difference of power in the top half of the core over that in the bottom half). A comparatively large xenon transient had been initiated. At this point the control part of the test was begun by manually moving the part length rods into the core. Control Group D was kept on automatic control and therefore moved out of the core to compensate for the reactivity worth of the part length rods as they were inserted into the core. When Control Group D reached 209 steps, a dilution was started to compensate for the remainder of the part length rod movement. Control Group D was then maintained at about the 209 step level for the rest of the test.

As the part length rods moved in, the axial power profile became skewed to the bottom of the core causing the axial offset to become progressively worse. However, at a position of approximately 120 steps the part length rods started pushing the flux to the top of the core. The axial offset had reached a maximum negative value of approximately -23% at this point. The time required for the part length rods to move from their starting position out of the core to the 120 step position was approximately 15 minutes.

The part length rods were then moved toward the bottom of the core in order to bring the axial offset to zero and completely

dampen the xenon transient. Approximately one hour later, the axial offset was exactly zero and the part length rods were at 70 steps. Control Group D was at 203.5 steps.

The axial offset was maintained at approximately zero for the next 24 hours until the test was terminated. The axial power profile and the corresponding axial offset were very sensitive to movement of the part length rods during this period. As little as a one step movement with the part length rods was noticeable on the two pen ΔI recorder. Consequently, the axial offset was easily maintained close to zero and did not exceed $\pm 3\%$. The only deviation from this limit occurred during a turbine runback when the axial offset went to -6% . The part length control rod position during the 24 hour period varied from 70 steps to 84 steps.

2.1.3 Experimental Data

Excure detector readings from the NIS meters were obtained hourly during the xenon transient tests along with heat balance measurements on the secondary side of the steam generators. Figure 1 shows the axial offset of power versus time for Phase I of the first test.

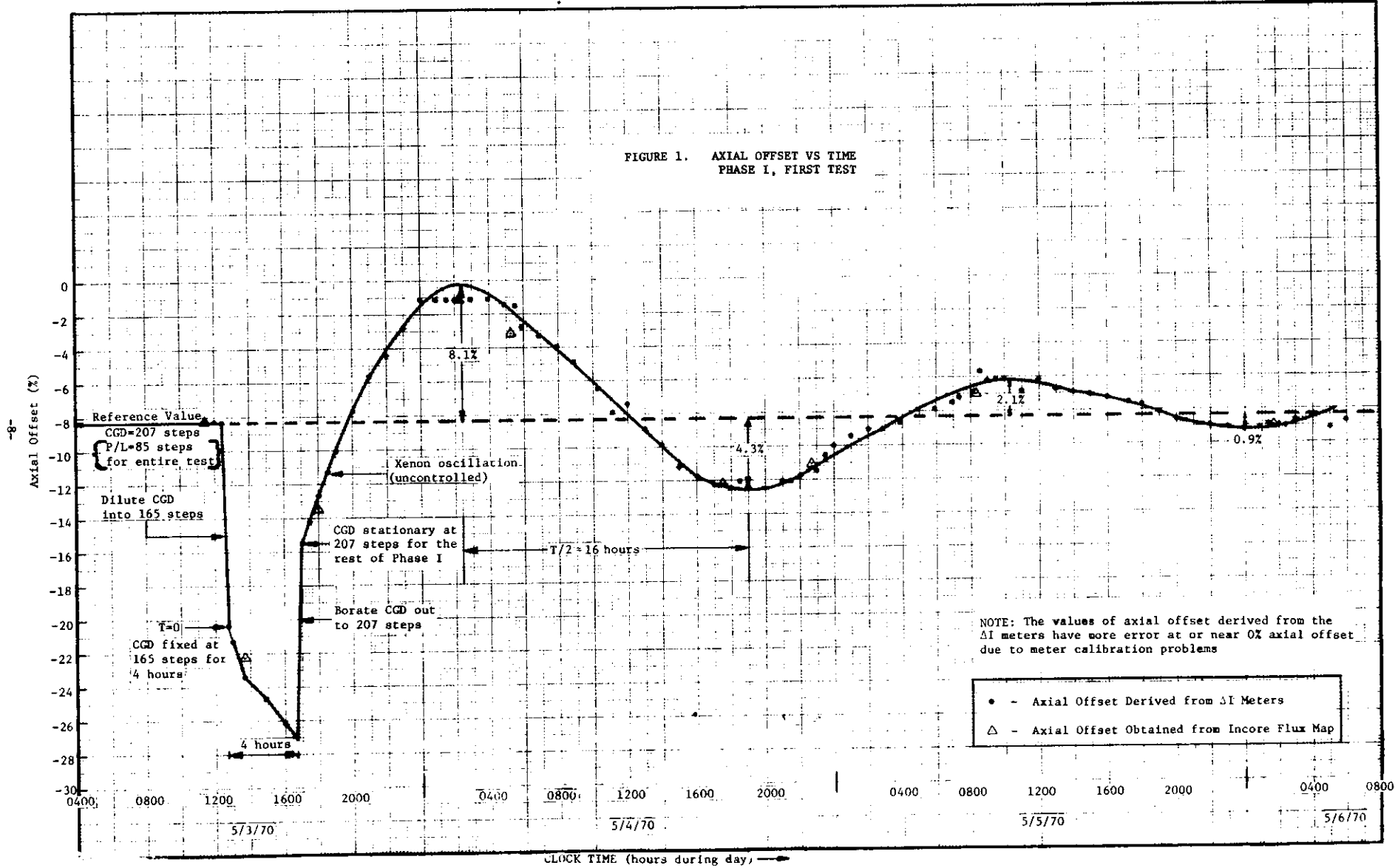
The axial offset values obtained from the ΔI readings were calculated according to the following equation:

$$A.O. = \frac{\Delta I (\%)}{\text{Fraction of Full Power}} \quad (1)$$

The values for fraction of power used in this equation were in all cases derived from secondary plant calorimetric data. The values of axial offset obtained from the ΔI readings are expected to represent the average actual incore axial offset to within approximately 1%.

The output currents from the ion chambers were also read every two minutes by the P-250 data logger during Phase I of the first

FIGURE 1. AXIAL OFFSET VS TIME
PHASE I, FIRST TEST



NOTE: The values of axial offset derived from the ΔI meters have more error at or near 0% axial offset due to meter calibration problems

- - Axial Offset Derived from ΔI Meters
- Δ - Axial Offset Obtained from Incore Flux Map

CLOCK TIME (hours during day) →

test. These data were then filtered through a low pass filter and normalized to the sum of all the top and bottom currents. This normalization corresponds to a power normalization as in Equation (1) above. The final ion current data for three pairs of detectors are shown in Figures 2 through 7.

Plots of percent power, part length rod position, Control Group D position and axial offset as a function of time for Phase II of the first test are presented in Figure 8.

2.2 Second Test at A Burnup of 7700 MWD/T

Due to Rochester Gas and Electric Corporation's power production commitments, all testing was performed at full power (1300 MWt), and, in order to avoid a turbine runback initiated by the Overpower ΔT protection system, axial offsets were procedurally limited to +15%. (At full power a turbine runback would have been initiated if the axial offset had exceeded +22%). Due to these restrictions, the induced perturbation of the axial power and xenon distributions was reduced from a 40 step insertion of bank D for four hours to a 25 step insertion of bank D for 50 minutes.

On February 16, 1971, the RGE reactor power was reduced to 75% and the part length bank was inserted to the core midplane (85 steps). Full power operation was then resumed. During preparations to begin testing, five days later, it was revealed by the two-pen strip chart recordings of excore detector data that the axial power oscillation introduced by the part length bank insertion had not completely dampened.

It was decided to proceed with the test and to superimpose a larger axial xenon oscillation over the smaller one. The oscillation

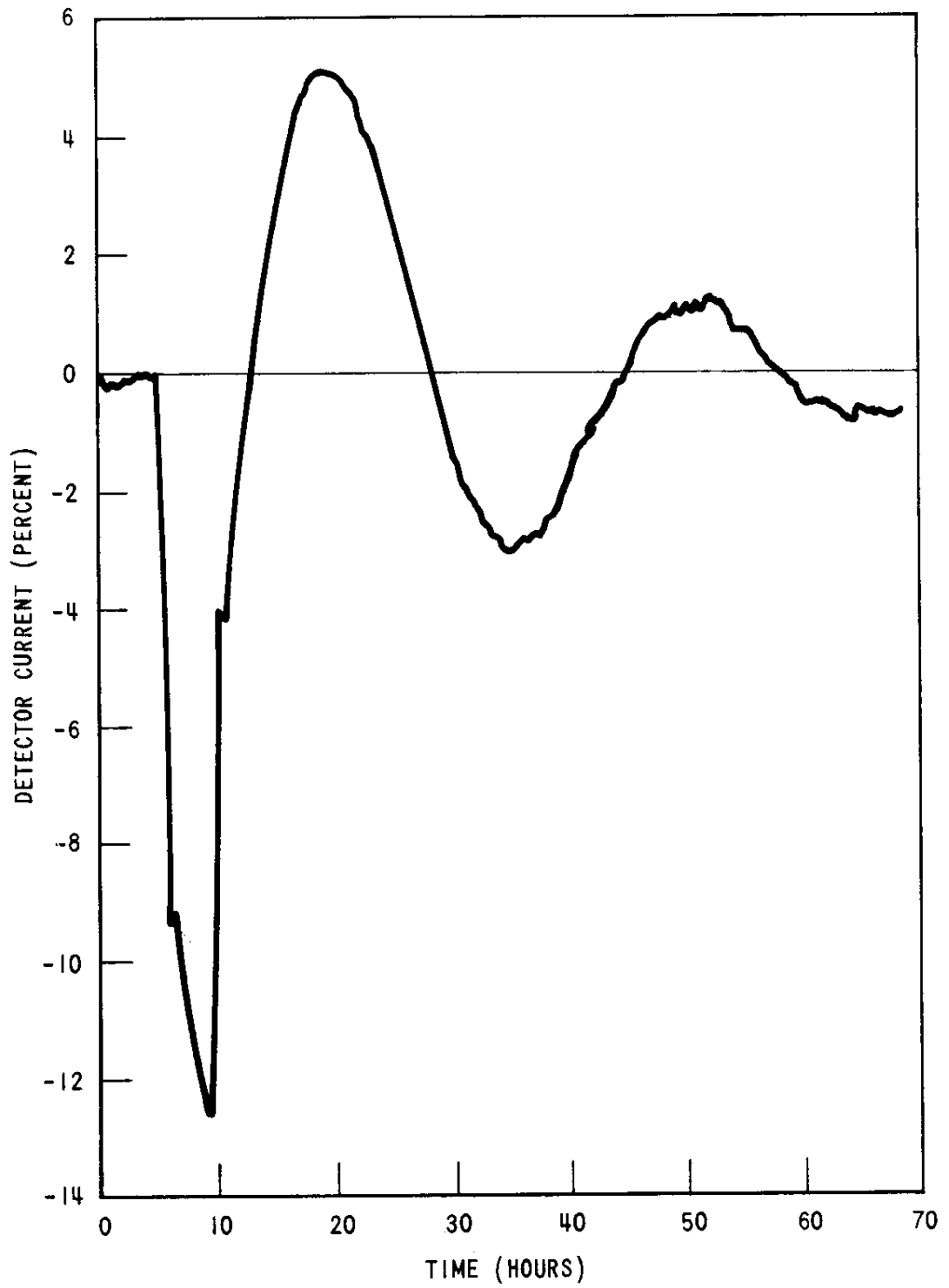


Figure 2. Detector Current from Channel 41A, Phase I, First Test

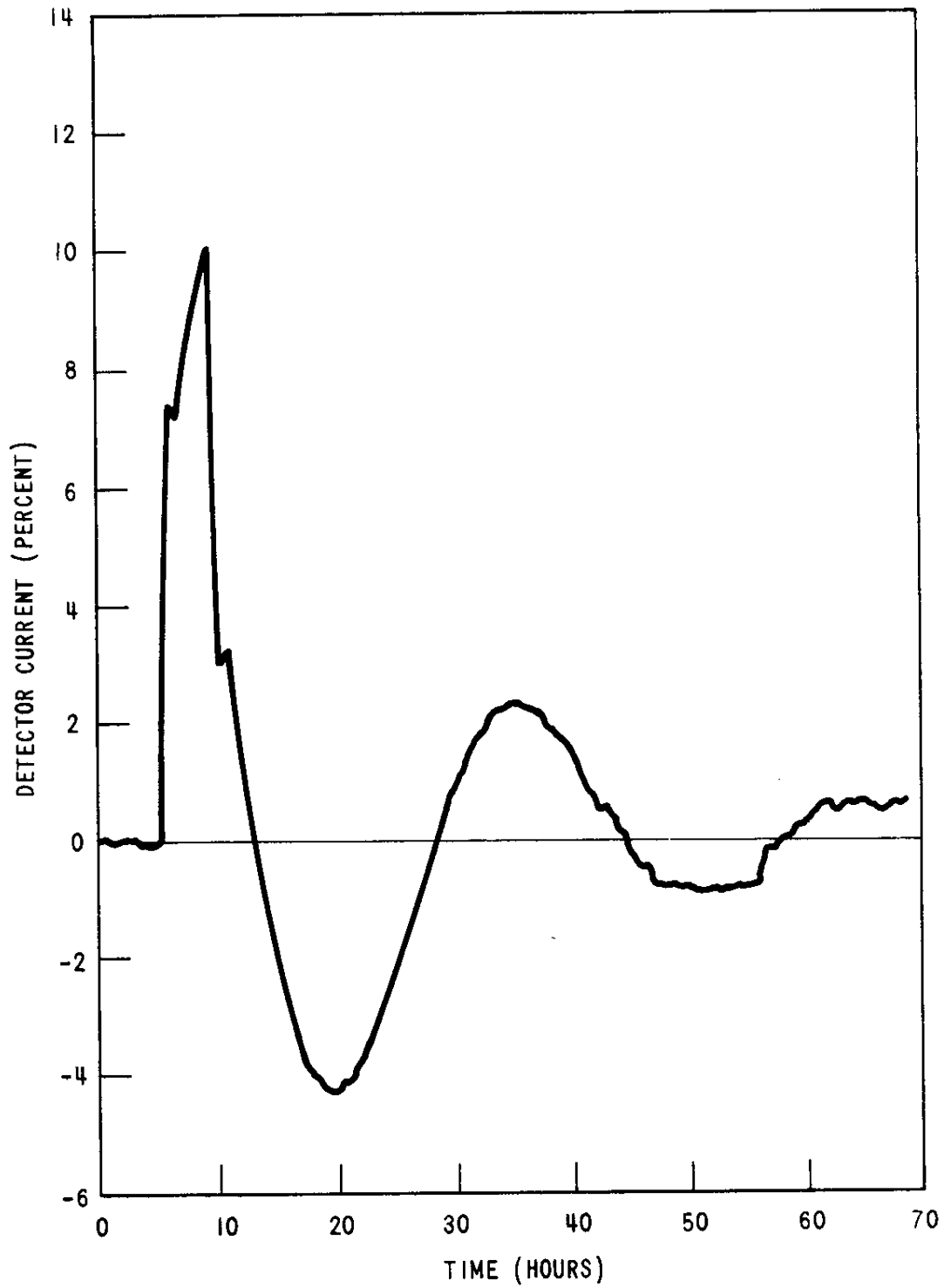


Figure 3. Detector Current from Channel 42A, Phase I, First Test

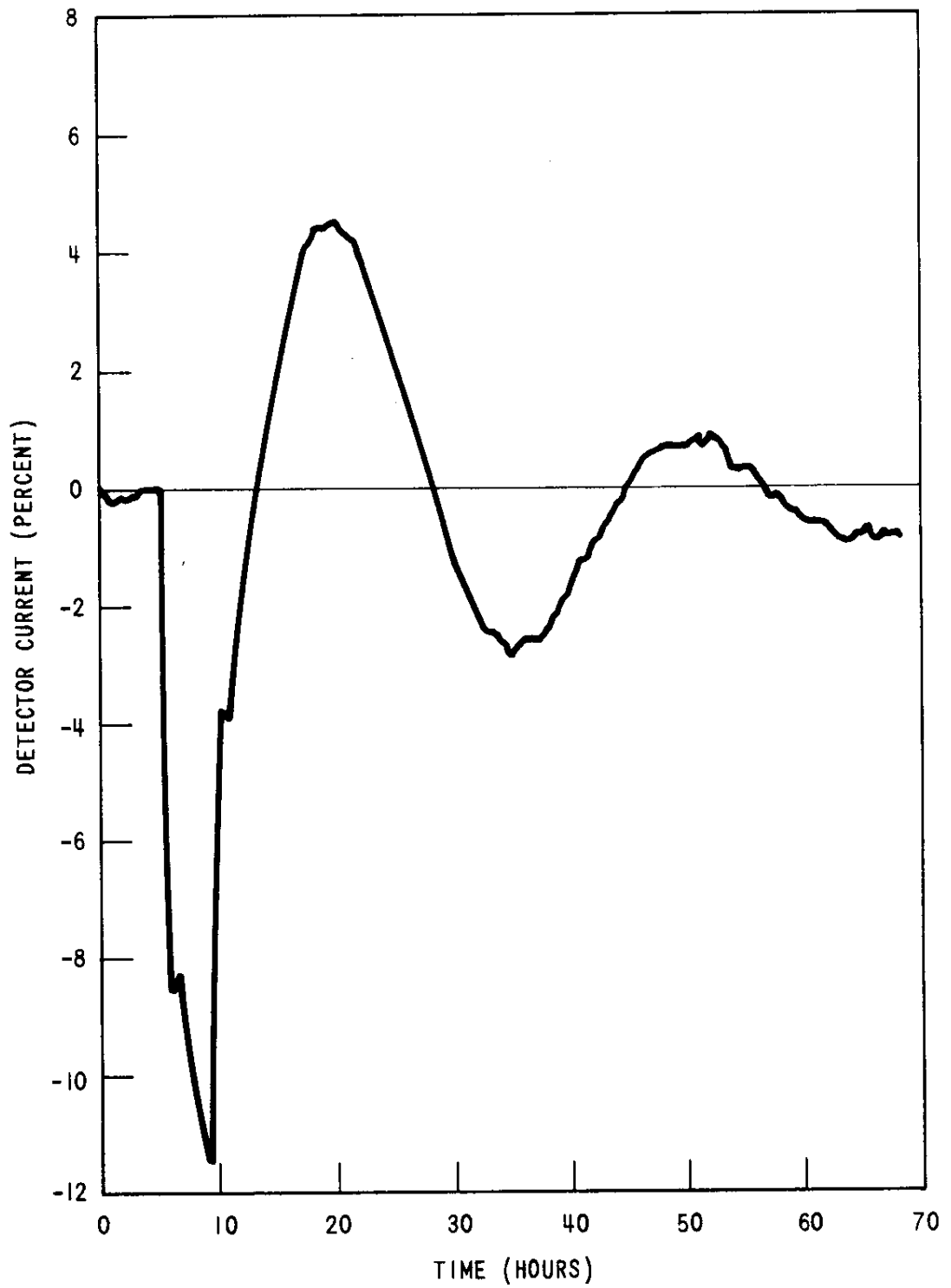


Figure 4. Detector Current from Channel 43A, Phase I, First Test

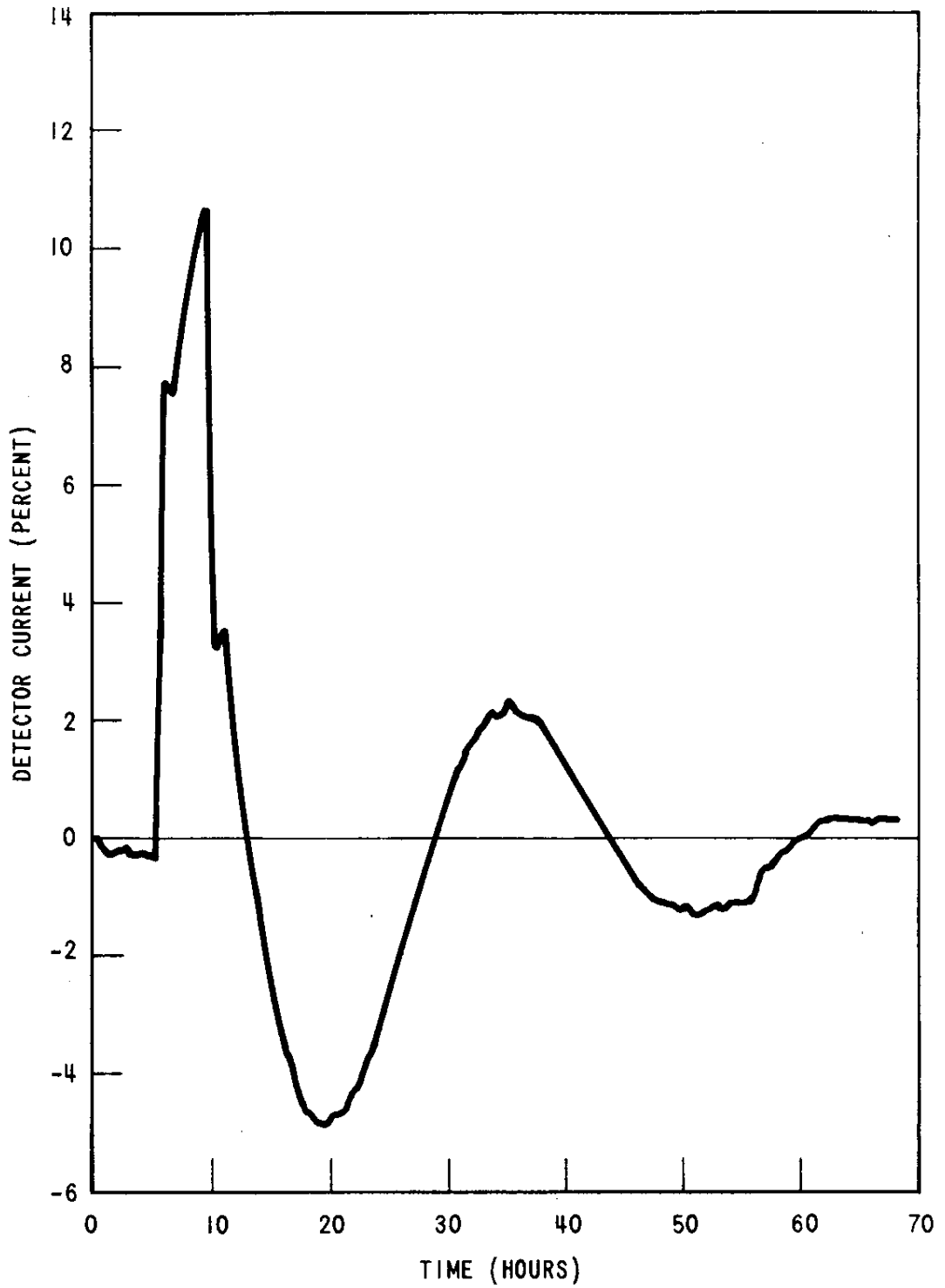


Figure 5. Detector Current from Channel 44A, Phase I, First Test

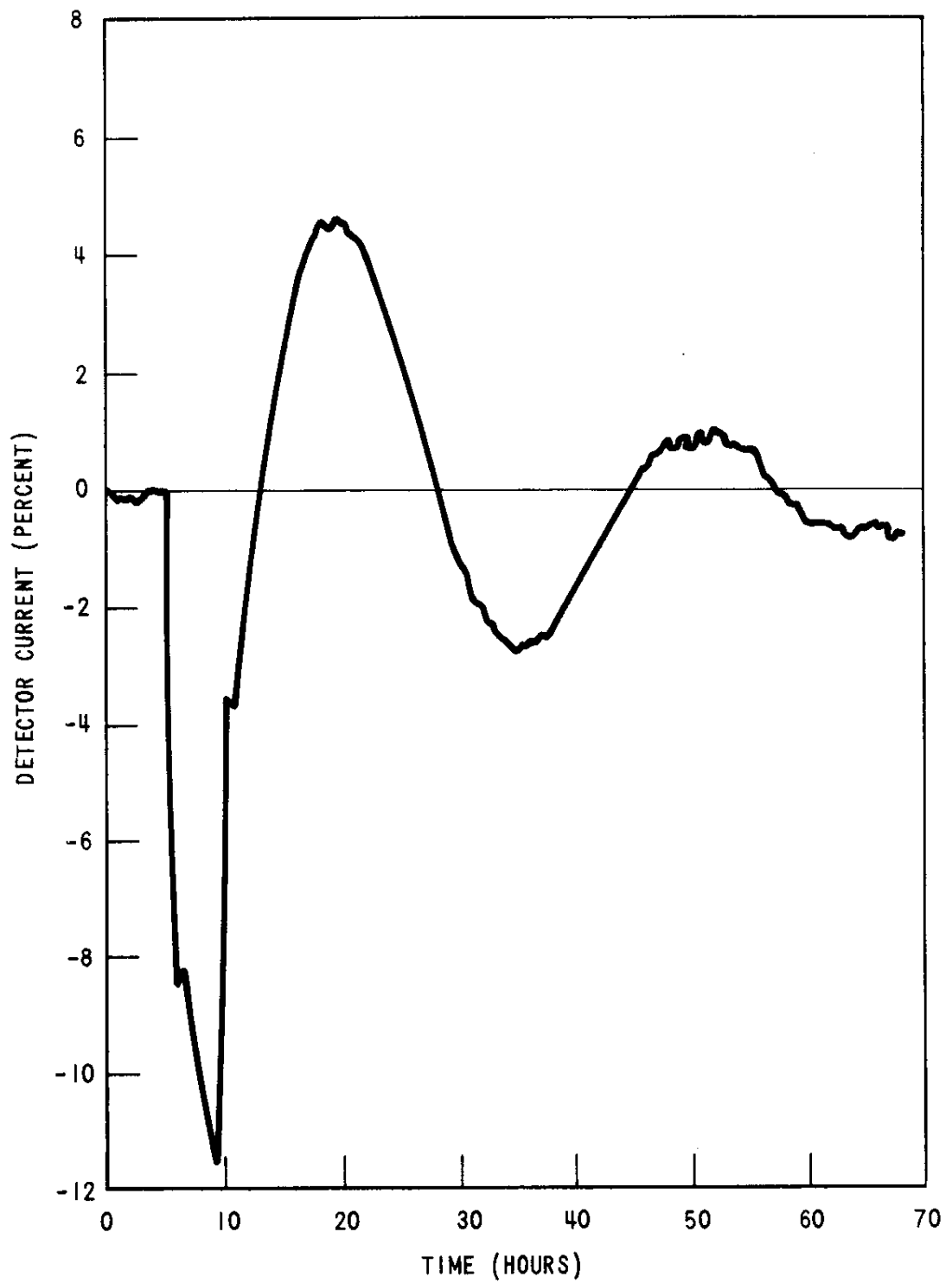


Figure 6. Detector Current from Channel 45A, Phase I, First Test

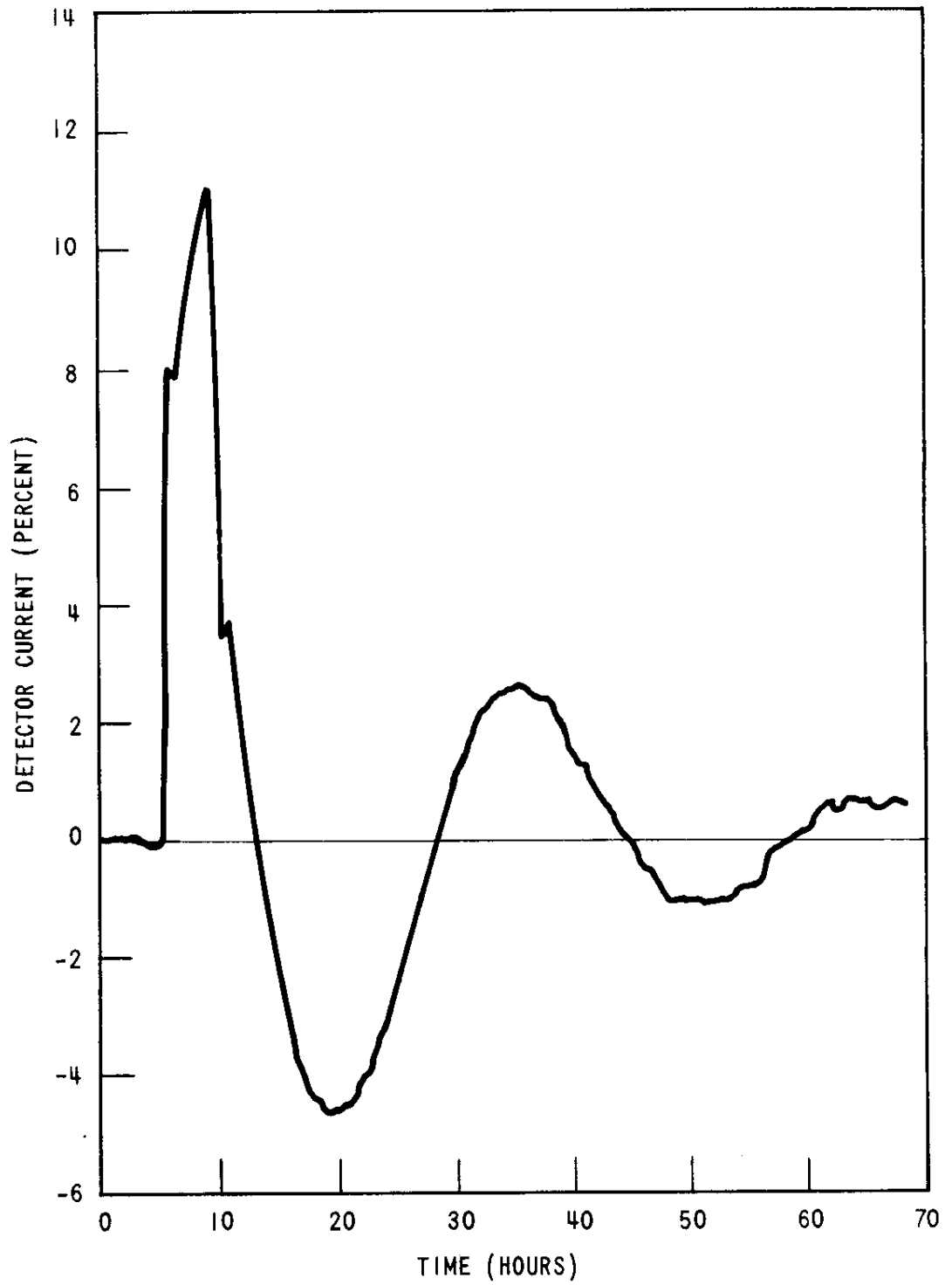


Figure 7. Detector Current from Channel 46A, Phase I, First Test

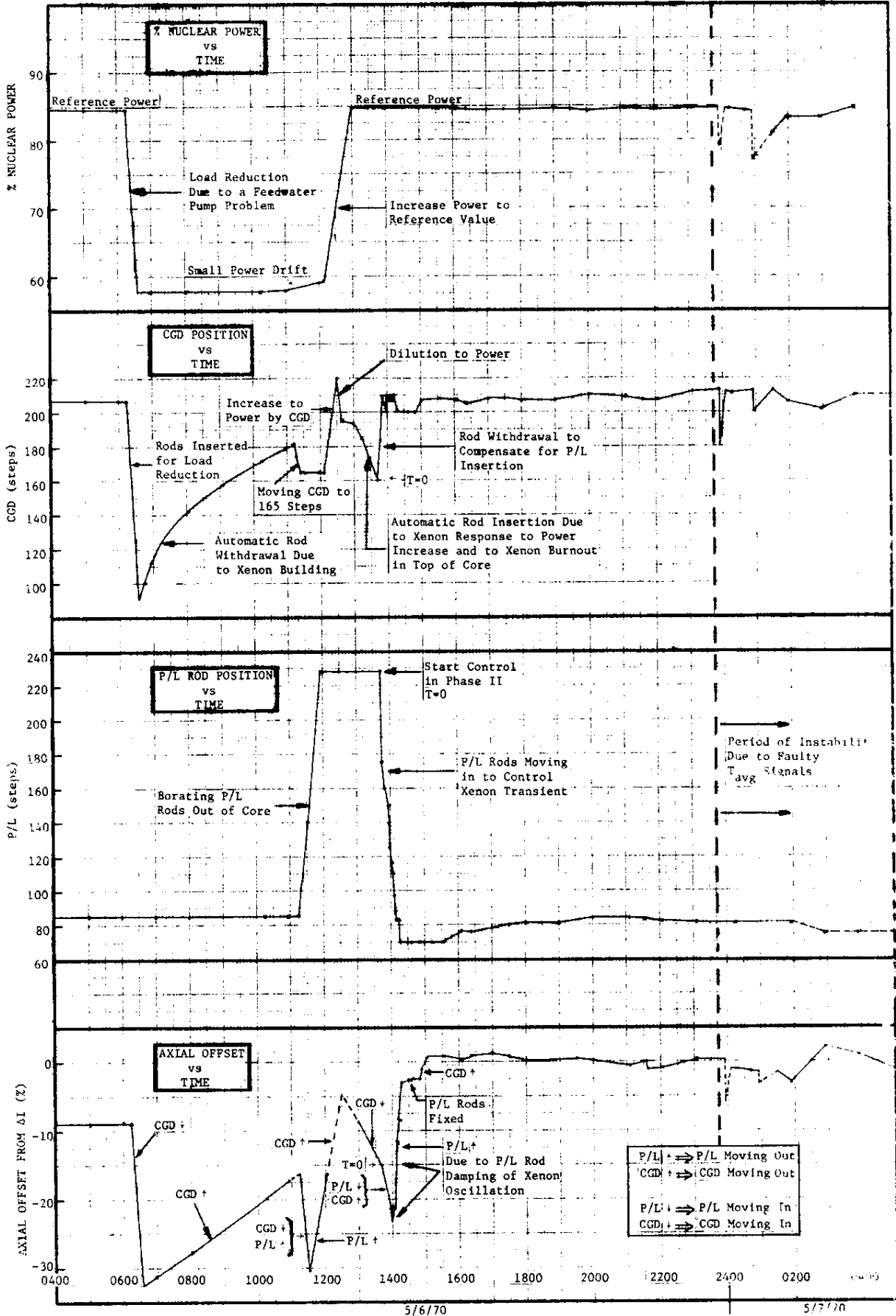


FIGURE 8. POWER, BANK D, P/L AND AXIAL OFFSET VS TIME, PHASE II, FIRST TEST

in progress would not interfere significantly with the intended purposes of this test. Proper handling of axial xenon-induced oscillation data which consists of two superimposed xenon transients with the same equilibrium conditions would still render the period and stability index of a clean, uncontrolled xenon oscillation characteristic of the core at that time in core life.

For 66 hours thermal power level, control bank positions and excore detector output were monitored on an hourly basis and incore flux maps were obtained at the extremum points in axial offset (maxima and minima).

Figure 9 illustrates Control Group D position and axial offset vs. time during the perturbation introduced for the second xenon test. Throughout the second test, conducted at an average burnup of 7700 MWD/T, nine incore flux maps were obtained. Axial offset of power data obtained hourly from the excore detectors were calibrated against incore results. These calibrated axial offset data are plotted in Figure 10, together with a curve obtained through a least-square-error fit.

Figure 11 shows the axial offset data obtained both before and during the second xenon stability test. These data points were obtained from strip chart recordings of excore detector data. The error incurred by extracting axial offsets from these recordings is significant for axial offsets close to 0% (as much as $\pm 1.0\%$ in axial offset). Therefore, nothing more than a most general trend should be interpreted from these results.

Axial offset data from the two xenon transient tests are shown in Figure 12. Figure 13 provides a comparison of the core average axial power distributions of the equilibrium conditions for the two oscillation tests. It is apparent from Figure 13 that Curve 2 at a burnup of 7700 MWD/T represents a flatter axial power distribution.

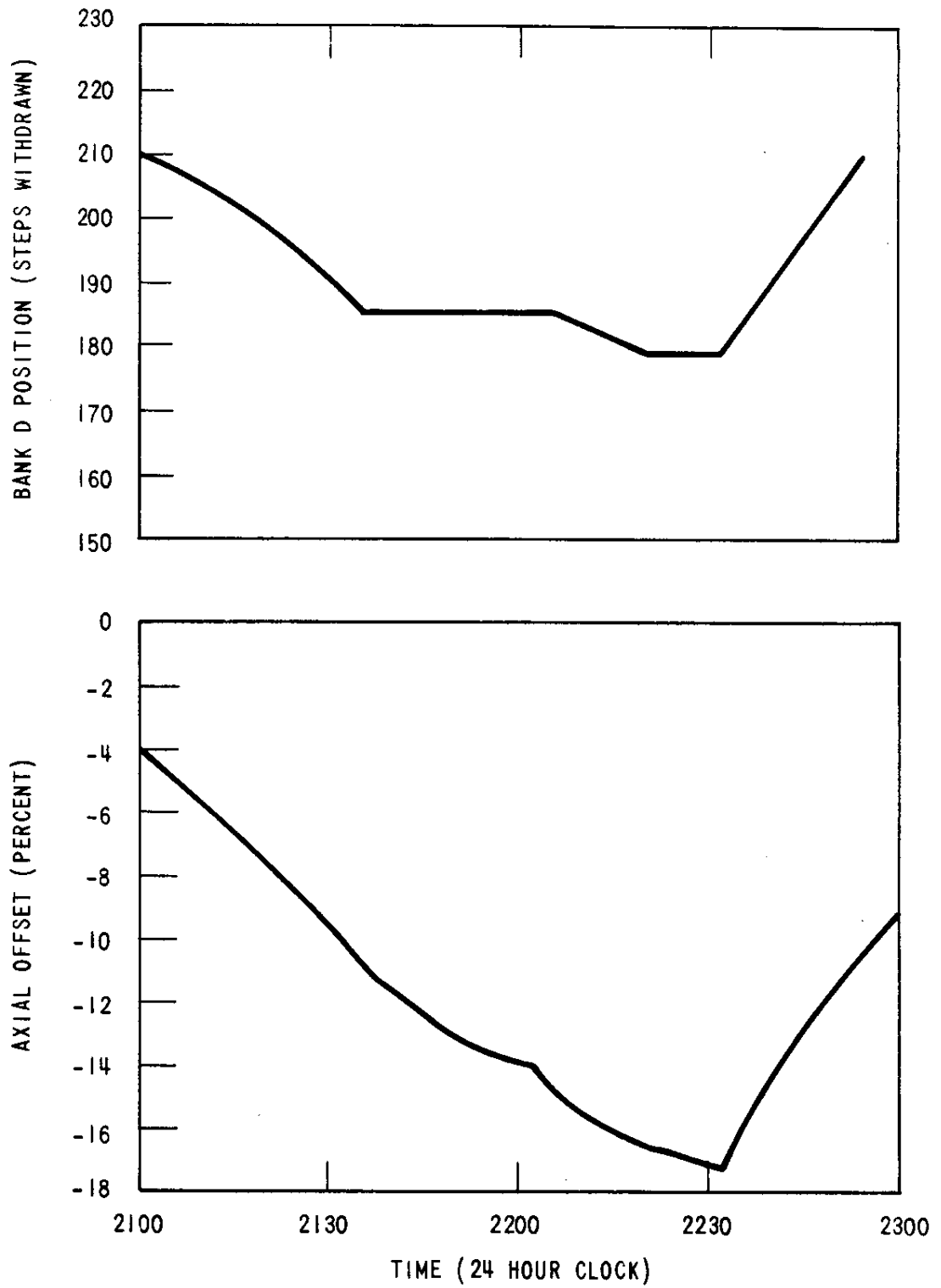


Figure 9. Bank D and Axial Offset versus Time During Perturbation, Second Test

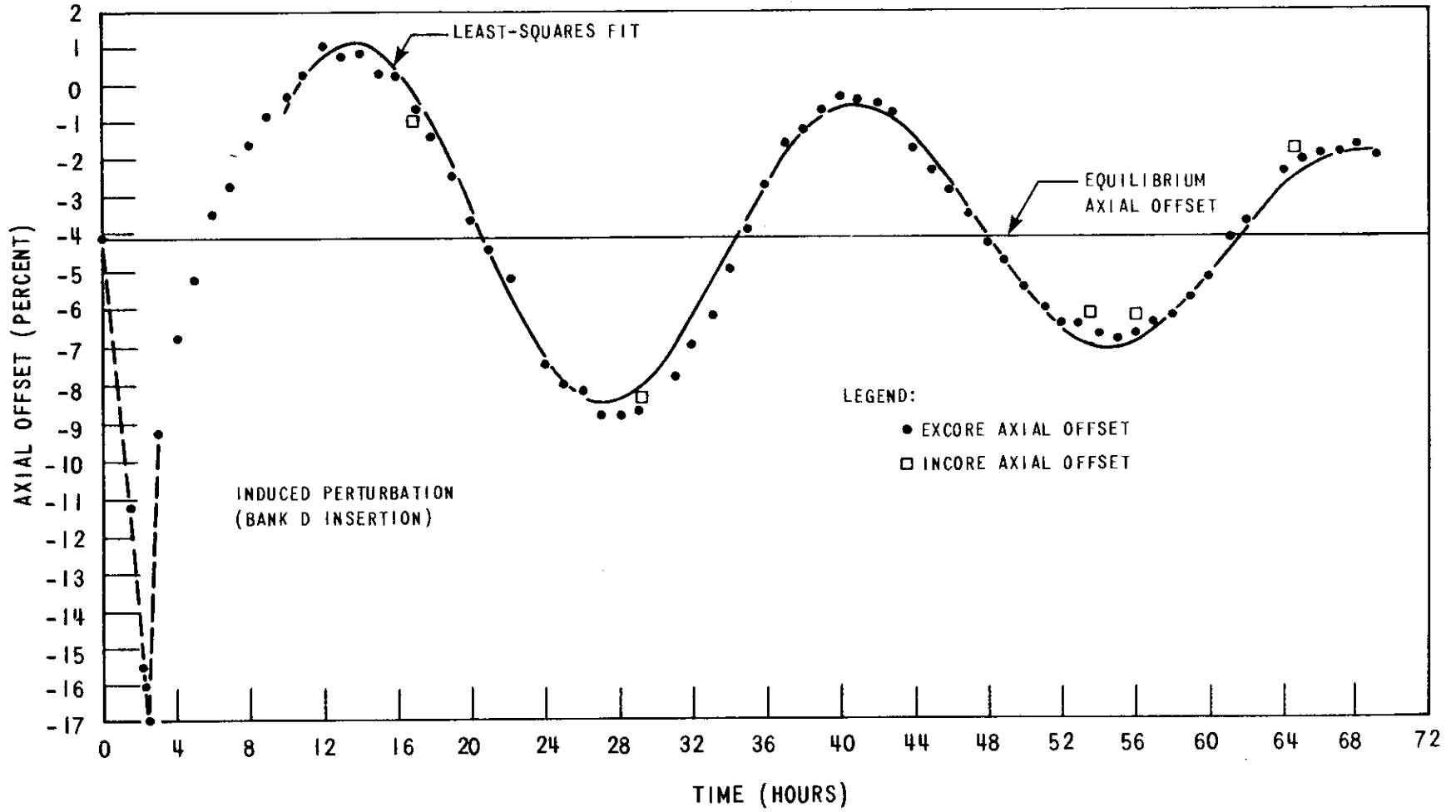


Figure 10. Axial Offset versus Time, Second Test

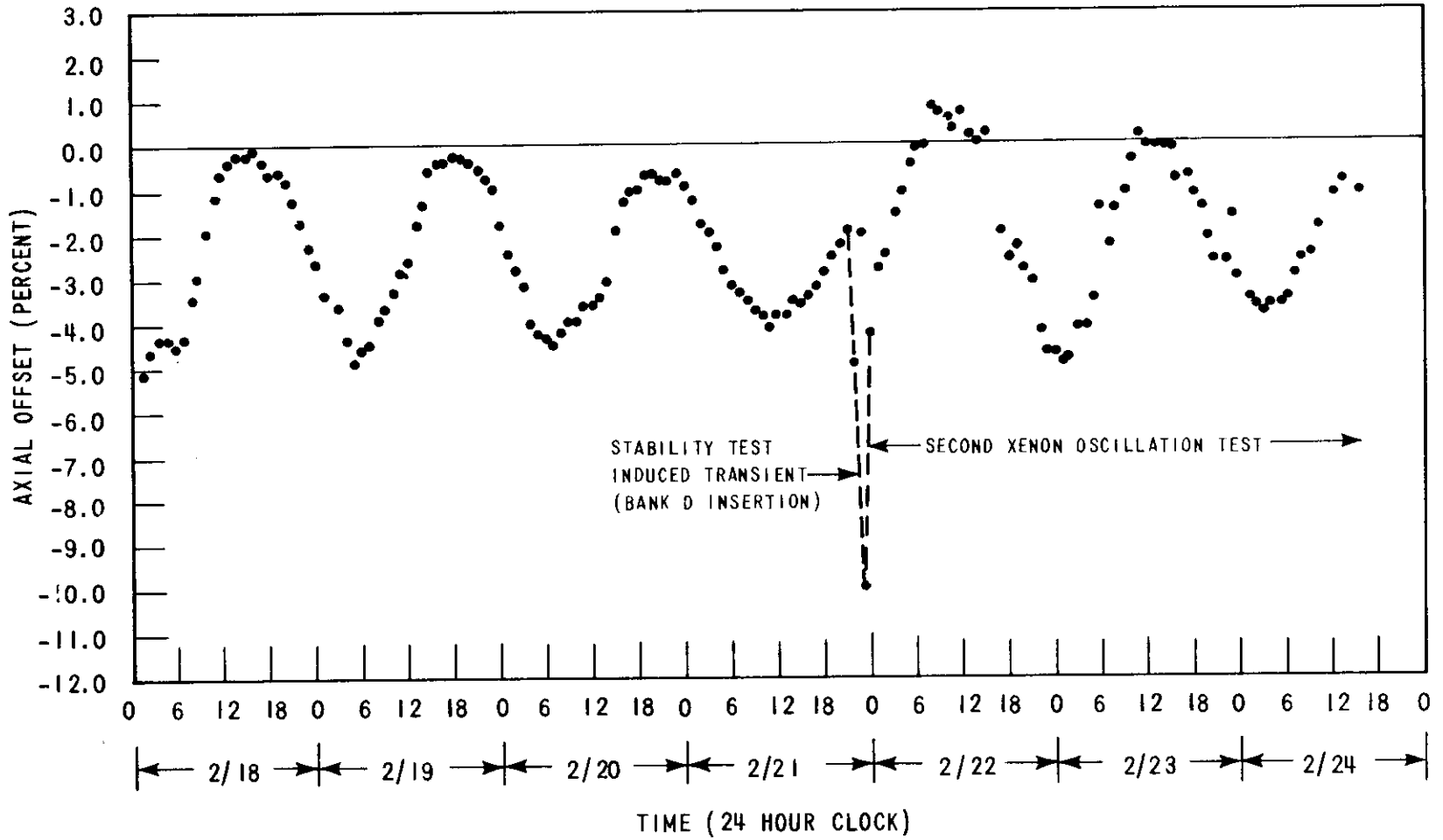


Figure 11. Axial Offset Data from Channel NE42, Second Test (Raw Strip Chart Data)

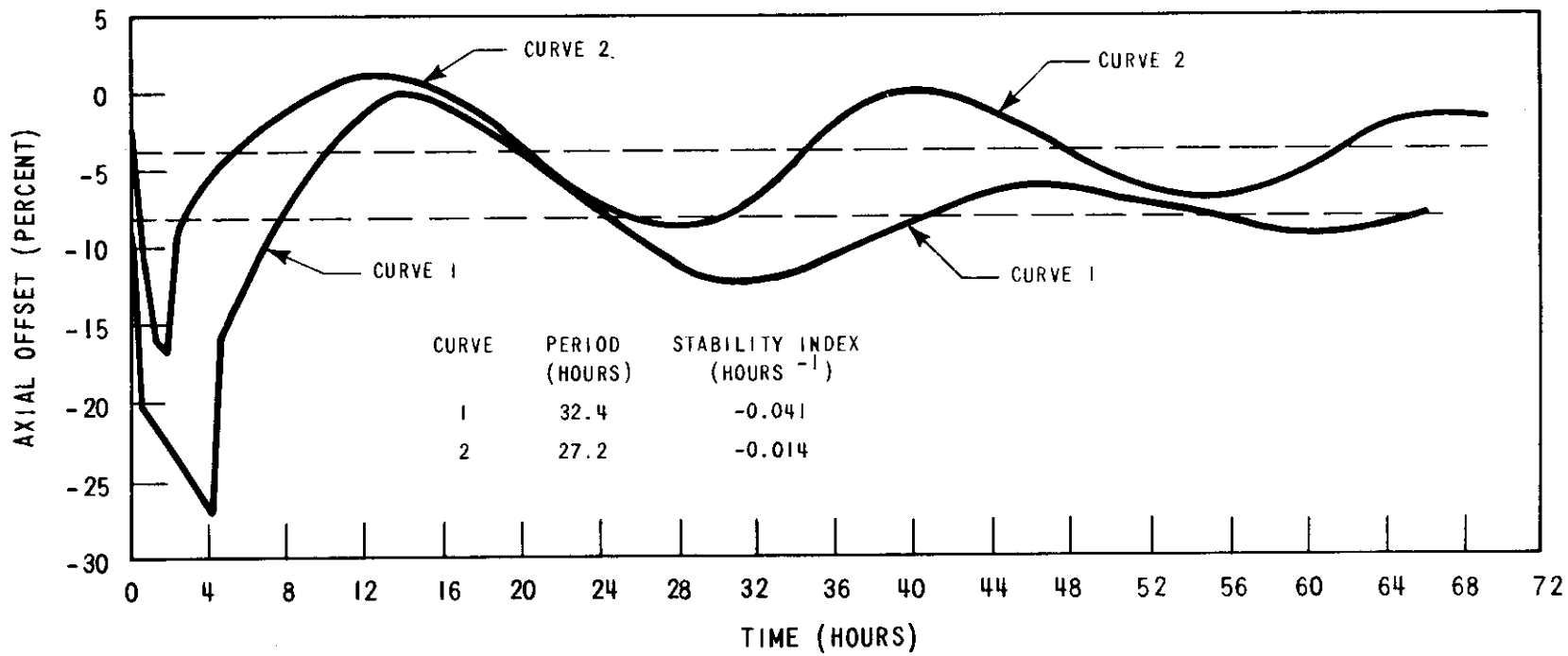


Figure 12. Axial Offset versus Time

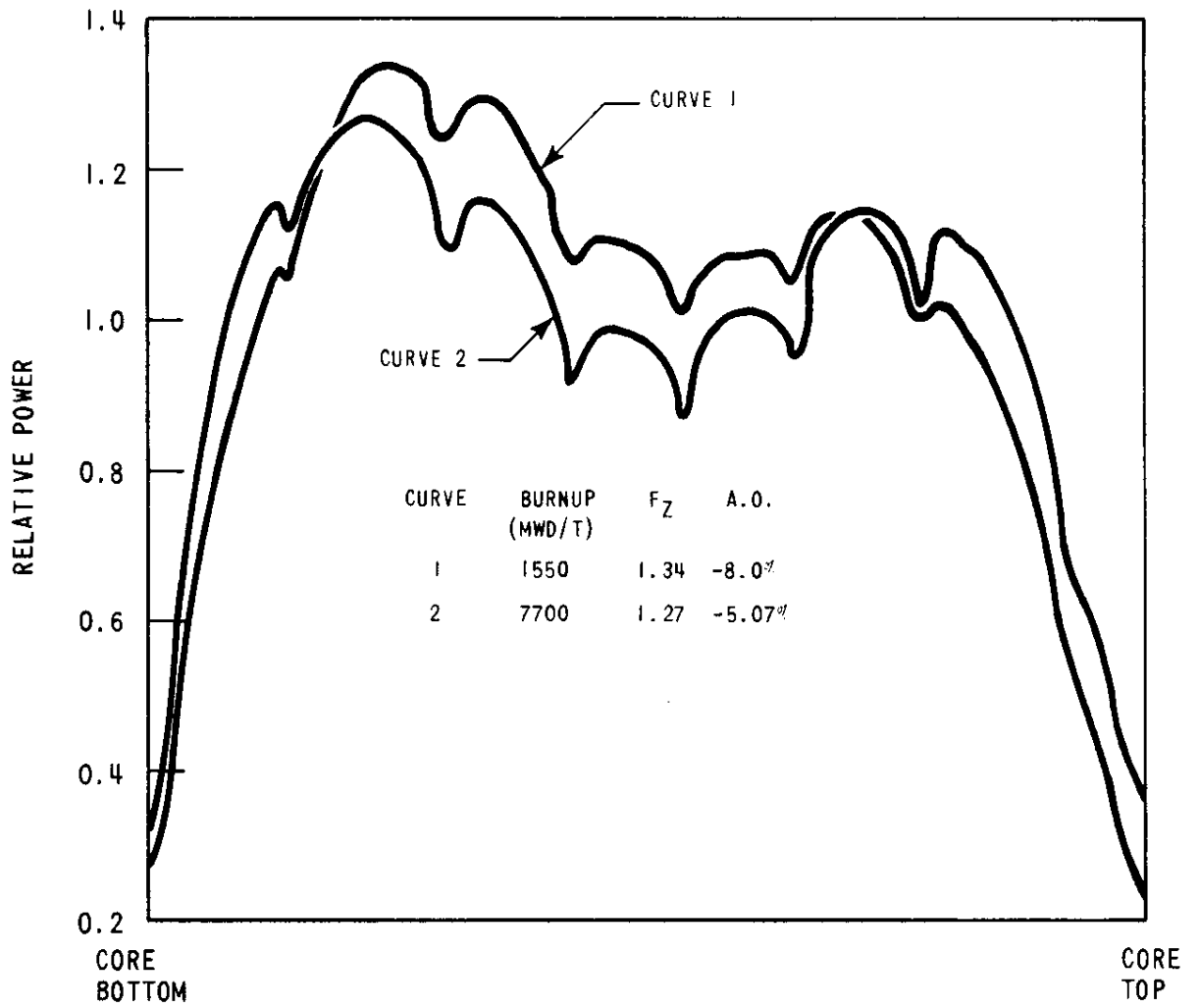


Figure 13. Average Axial Power Distribution

SECTION 3

STABILITY INDEX FROM THE EXPERIMENTAL DATA

3.1 The Concept of the Stability Index

Since in practice we are often interested in the stability of the first flux harmonic, we would like to obtain the eigenvalue ξ_1 of that overtone. The eigenvalue ξ_1 is, in general, a complex number, i.e.,

$$\xi_1 = b_1 + i c_1 \quad (2)$$

where b_1 is defined as the stability index and $2\pi/c_1$ the oscillation period of the first harmonic. By obtaining the axial offset of power while maintaining the total power constant we can essentially eliminate the contributions from all even harmonics including the fundamental and the second modes, and obtain the eigenvalue ξ_1 to a good approximation. Equation (2) implies that in the time domain the AO of power as a function of time t can be expressed as

$$AO(t) = A_1 e^{\xi_1 t} = a_1 e^{b_1 t} \cos c_1 t, \quad (3)$$

where A_1 and a_1 are constants. Using Equation (3), the stability index b_1 and the period $2\pi/c_1$ can be obtained from a least-square-error fit of the AO data. They can also be obtained approximately by comparing AO at the extremum points.

3.2 Results of the First Test

For Phase I of the first RGE test conducted at a core average burnup of 1550 MWD/T, the stability indices and the periods were calculated for the normalized current data from each of the three pairs of top and bottom detectors as shown in Figures 2 through 7. The results are presented in Table 1. Here Equation (3) was used at two successive peaks to calculate the stability indices. Included also in Table 1 are the stability index and the period calculated from the average AO of power data shown in Figure 1 through a least-square-error fit. It is to be noted that the stability indices and periods obtained from the two methods are in satisfactory agreement.

3.3 Results of the Second Test

As mentioned earlier in Section 2.2, for the second RGE test, it was observed that a perturbation in the form of an impulse motion of Control Group D was introduced in a core which was already undergoing a small oscillation induced by PL rod insertion a few days before the test. It was assumed in the analysis of the data that the transient introduced by PL insertion was undergoing an oscillation during the test with nearly the same equilibrium condition as that for the oscillation introduced by Group D insertion. That is, the two oscillations are assumed to have the same eigenvalue, ξ_1 . Then the composite transient will be represented by the same eigenvalue, ξ_1 , as can be readily verified by combining two functions of the form given by Equation (3) but with different constants a_1 and A_1 . A least-square-error fit was run using Equation (3) for the composite data as shown in Figure 10 to obtain the stability index and the period. The results are presented in Table 2 along with the axial hot channel factor and the AO for the equilibrium power distribution and are compared with corresponding data from the first test.

TABLE 1

Stability Index and Period for the First RGE Test

	<u>Data Source</u>	<u>Stability Index (hr⁻¹)</u>	<u>Period (hrs.)</u>
	41A-1 Top	-0.035	31.2
	42A-1 Bottom	-0.041	32.0
Detector	43A-2 Top	-0.031	32.0
Current	44A-2 Bottom	-0.046	31.6
	45A-3 Top	-0.033	31.8
	46A-3 Bottom	-0.036	32.0
Axial Offset of Power		-0.041	32.4

TABLE 2

Comparison of the Two RGE Tests

<u>Burnup (MWD/T)</u>	<u>Axial Hot Channel Factor</u>	<u>Equilibrium A.O. (%)</u>	<u>Stability Index (hr⁻¹)</u>	<u>Period (hrs.)</u>
1550	1.34	-8.0	-0.041	32.4
7700	1.27	-5.1	-0.014	27.2

A trial was made to separate the two transients in the second test which were somewhat out of phase with one another. As mentioned in connection with Figure 11, however, the amplitudes of the oscillations involved were not large enough to insure sufficient accuracy in the AO data. Hence, a quantitative treatment of the data was limited to the composite transient.

SECTION 4

ANALYSIS OF THE TESTS

4.1 Calculational Model

The calculations were performed in an axial slab geometry using a flux synthesis technique, where the radial weighting factor for the Doppler feedback was obtained as a function of power and burnup. The direct simulation of axial offset data was carried out using the PANDA Code^[2], which solves the two-group, time-independent neutron diffusion equation with time-dependent xenon and iodine concentrations. The stability index was also calculated by using the PANDA-SPARTA^[3] link (HORACE). The code HORACE calculates space-dependent reactor transfer function in the Laplace transform domain using the two-group time-dependent neutron diffusion equation with time-dependent xenon and iodine concentrations. The fuel temperature and moderator density feedback is currently limited to steady-state model.

The nuclear cross-sections used in this study were generated from a unit cell depletion program which has evolved from the codes LEOPARD^[4] and CINDER^[5], and the plant follow data were closely simulated.

For the direct PANDA calculation, by obtaining the axial offset of power while maintaining the total power constant, we can essentially eliminate the contributions from all even harmonics of flux, including the fundamental and the second modes, and obtain the eigenvalue ξ_1 of the first flux overtone through Equation (3).

In trying to obtain the same eigenvalue in the Laplace domain, using the concept of the space-dependent transfer function, the contamination from even harmonics can be minimized by introducing a spatially asymmetric perturbation source. It was found necessary in the present study to further eliminate the contamination from even harmonics, especially when the fundamental mode was not symmetric, by taking the axial offset of the calculated transfer function in the Laplace domain.

4.2 Results of Calculation

4.2.1 Core Stability Calculation

Stability indices were calculated for both of the RGE tests and are compared with the measured values in Table 3.

For the direct PANDA calculation, the stability index was calculated by using a least-square-error fit of Equation (3) through the calculated AO of power. The calculated stability index was further corrected to that corresponding to a zero time-step length^[6]. A similar time-step length correction on the calculated oscillation period was made at the rate of 3.5 hours reduction in the period per hour of time-step^[7]. The PANDA-SPARTA (HORACE) calculation has a tendency to predict a higher degree of stability compared to the direct PANDA calculation, but the agreement between them is regarded as acceptable at this point, especially under the presence of fairly large experimental uncertainties.

The Doppler coefficient model used for this study is based on a fuel temperature model that includes burnup-dependent behaviors of fuel pellets. Model C calculates the gap conductance based on a closed gap model, whereas Model H uses a burnup-dependent gap conductance model. Model C gave good agreement with the measured stability index in Phase I of the first test. Hence, the Model C temperature model was used to simulate Phase II of the first test. For the rest of the calculation, Model H was used.

TABLE 3

RGE Stability Index Calculation

<u>Case</u>	<u>Burnup (MWD/T)</u>	<u>PL</u>	<u>Power</u>	<u>Means of Evaluation</u>	<u>Parameters</u>	<u>Stability Index (hr⁻¹)</u>	<u>Period (hrs.)</u>
1	1550	Center	85%	Experiment		-0.041	32.4
2	1550	Center	85%	PANDA	Model H Temperature	-0.030 (-0.032)*	34.2 (32.4)*
3	1550	Center	85%	HORACE	Model H Temperature	-0.044	29.7
4	1550	Center	85%	PANDA	Model C Temperature	-0.041 (-0.044)*	34.9 (33.1)*
5	1550	Center	85%	HORACE	Model H, ENDF Xenon	-0.060	31.9
6	1550	Out	85%	HORACE	Model H Temperature	-0.080	31.7
7	7700	Center	100%	Experiment		-0.014	27.2
8	7700	Center	100%	PANDA	Model H Temperature	-0.006 (-0.006)*	32.8 (31.0)*
9	7700	Center	100%	HORACE	Model H Temperature	-0.006	29.2
10	7700	~Center	100%	HORACE	Model H, Power Distribution Matched	-0.017	29.9
11	7700	Center	100%	HORACE	Model H, ENDF Xenon	-0.019	30.0
12	7700	Out	100%	HORACE	Model H Temperature	-0.028	30.1
13	7700	Center	85%	HORACE	Model H at 1550 MWD/T	+0.017	29.6
14	7700	Center	85%	HORACE	Model H and Boron at 1550 MWD/T	+0.005	30.9

* Numbers in the parentheses indicate those corrected to zero time-step length.

Calculation of the stability indices based on the Model H temperature model as shown in Table 3 yields conservative results compared to experiments with a margin of approximately -0.01 hr^{-1} in the stability index. It was suspected that the disagreement between the calculation and the experiment at a burnup of 7700 MWD/T could be partly due to mismatch in power distribution at that burnup (Cases 8 and 9 in Table 3). Calculated power distributions are somewhat more dipped than measured near the core midplane where the PL rods are inserted. A trial was made to more nearly match the power distribution obtained from the incore flux maps by an arbitrary adjustment of the PL rod absorption cross-section and position (Case 10 of Table 3). This calculation shows that the mismatch in the power distribution could result in an error in the stability index of approximately 0.01 hr^{-1} . Due to uncertainties in the Doppler coefficient model, a further trial to match the measured stability indices was not made.

In order to assess the relative influence of the several effects of fuel burnup on the core stability, a few parametric variations were made with the HORACE code.

1. Effect of change in Doppler coefficient: The Model H temperature used for this analysis predicts that the negative Doppler coefficient around full power tends to increase somewhat in magnitude as fuel burnup progresses. In Case 13 of Table 3 the Doppler coefficient at a burnup of 1550 MWD/T was used with burnup and power distributions at 7700 MWD/T. A comparison of Cases 13 and 9 shows that this change in Doppler coefficient could account for a change of approximately -0.02 hr^{-1} in stability index.
2. Effect of decrease in critical boron concentration: As fuel burnup progresses, the critical boron concentration decreases,

resulting in a more negative slope of the moderator temperature coefficient curve as well as a more negative temperature coefficient itself. This increase in magnitude of the negative derivative of the moderator temperature coefficient with respect to the moderator temperature has a destabilizing effect on the first flux harmonic. In Case 14 of Table 3 we used the 1550 MWD/T Doppler coefficient and increased the boron concentration from 700 ppm to 1065 ppm, while maintaining the burnup and power distributions of 7700 MWD/T. A comparison of Cases 13 and 14 shows that this change in the slope of the moderator temperature coefficient could account for approximately $+0.01 \text{ hr}^{-1}$ in the stability index.

3. Effect of power flattening: As shown in Figure 13, as fuel burnup progresses, the axial power distribution becomes flatter. Since we have to admit a certain amount of uncertainty due to disagreement between the PANDA and HORACE codes and to compensate for the effect of the mismatch in power distribution, Case 14 was compared with Cases 2 and 3 as a basis for evaluating the effect of power flattening. A change of $+0.035 \text{ hr}^{-1}$ in stability index is estimated as the power flattening effect.

The sum of the three effects above results in a net change of $+0.025 \text{ hr}^{-1}$ in the stability index due to fuel depletion from an average burnup of 1550 MWD/T to 7700 MWD/T.

The microscopic xenon absorption cross-section used in this study is from the TEMPEST Library^[8]. The use of xenon cross-sections from the ENDF/B-II Library^[9] tends to slightly overpredict the core stability (Cases 5 and 11) for the RGE tests.

The insertion of PL rods at the core center makes the core less stable due to flattening of the axial power distribution as shown in Cases 6 and 12 in Table 3.

4.2.2 Direct Simulation of the Tests

Figure 14 shows the comparison between the experimental axial offset data and the calculated values for Phase I of the first test. Even though the agreement with the experimental stability index value is reasonable for both of the temperature models, the simulation of the axial offset data is not so good, due in part to the use of a finite time-step size. It was also suspected that due to an earlier impulse test, aborted halfway (Section 2.1.1), the xenon concentration might not have been at the equilibrium value at the start of the Phase I test. A comparison similar to Figure 13 was obtained for the second test.

In Figure 15, we present the result of simulation of Phase II of the first test. In the first trial (Curve 1), the PL rods motion was smoothed out to within 5 steps. This resulted in rather a poor agreement with experimental data. The agreement became better in the next trial (Curve 2) when we followed the PL motion more closely. This is in agreement with the experimental observation that the effect of PL movement by a step was visible on the ion chamber recorders (Section 2.1.2). This sensitivity of the axial offset to PL motion is due to the saddle-shape of power and xenon distributions at the time the PL rods were inserted to the core center. A modification was made in the PANDA code in the present study so that a search could be made for axial offset by varying the PL position. A calculation using the modified version of PANDA shows that a continuous PL motion of up to 5 steps is necessary to maintain the axial offset at zero. The free-running oscillations (Curves 1 and 2, after $t = 24$ hours) show that without the small but continuous movement of PL, the transient could have gone through further oscillations. It was verified by the test, however, that the PL rods were effective in controlling the axial xenon oscillation.

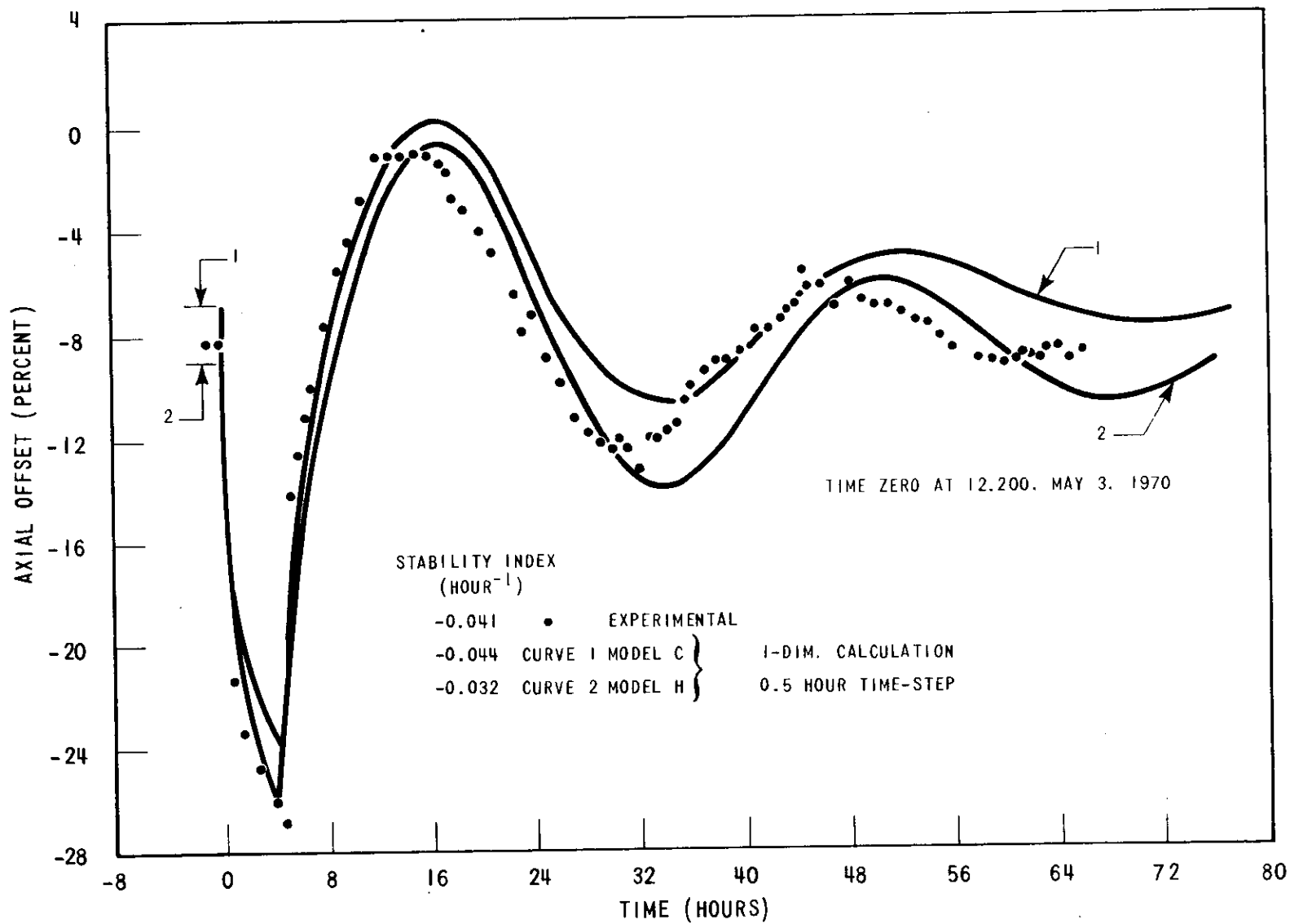


Figure 14. Axial Offset versus Time, Phase I, First Test

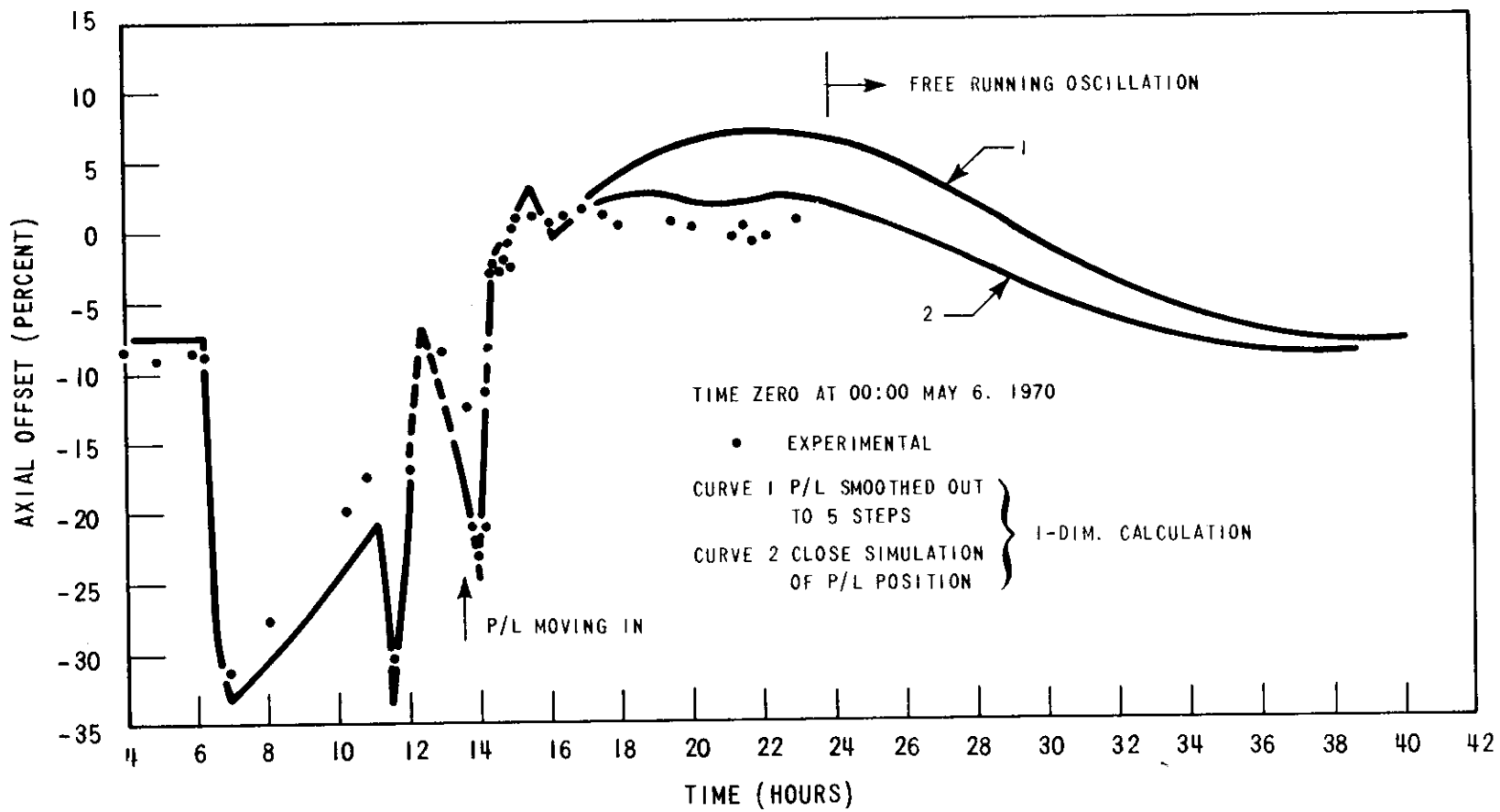


Figure 15. Axial Offset versus Time, Phase II, First Test

SECTION 5

CONCLUSIONS

As a follow-up of the CYW xenon transient tests^[1], two axial xenon transient tests were conducted at the RGE plant, the first at a core average burnup of 1550 MWD/T and the second at 7700 MWD/T, respectively. The stability indices and the oscillation periods were measured in uncontrolled, free-running oscillations. In the first test, a trial was also made to control an induced axial transient by the movement of the part length rod. Calculation of the stability indices and the direct simulation of the tests were also made.

The conclusions from the analysis of the tests are:

1. The RGE core was stable against induced axial xenon transients both at the core average burnups of 1550 MWD/T and 7700 MWD/T. The measured stability indices are -0.041 hr^{-1} for the first test (Curve 1 of Figure 12a) and -0.014 hr^{-1} for the second test (Curve 2 of Figure 12a). The corresponding oscillation periods are 32.4 hours and 27.2 hours, respectively. A stability index of -0.049 hr^{-1} and oscillation period of 30.0 hours were obtained in a similar test at CYW at the average burnup of 9290 MWD/T.
2. The excore detectors were adequate to monitor axial power distributions in a depleted core.
3. The PL rods were sufficient to shape the axial power profile and to dampen the axial xenon oscillations effectively.
4. The normal control board readout equipment available to the operator provided sufficient information to the operator for a rapid and effective PL rod control.

5. Core stability calculations yield conservative results for both of the RGE tests with a margin of approximately 0.01 hr^{-1} in the stability index.
6. The RGE tests show that the reactor core becomes less stable as fuel burnup progresses but that the RGE core was still stable at a burnup of 7700 MWD/T.
7. In PWR's of the RGE type, as full burnup progresses the power distribution becomes flatter, as shown in Figure 13, and the moderator temperature coefficient becomes more negative. Both the flatter power distribution and the more negative moderator temperature coefficient make the core less stable to axial xenon oscillations. The change in moderator temperature coefficient is destabilizing because the slope of the coefficient curve becomes more negative.
8. The Doppler coefficient model used for this analysis predicts that the negative Doppler coefficient around full power tends to increase somewhat in magnitude as fuel burnup progresses, which acts in the direction of reducing the other destabilizing effects of fuel burnup.

ACKNOWLEDGEMENT

The authors wish to thank the staff of the Rochester Gas and Electric Reactor Facility, in particular to Mr. William L. McCoy, for their help and cooperation in the conduct of the tests. The first author (John C. Lee) also wants to thank Mr. I. Elmer Dominick for his valuable assistance at various stages of the simulation and analysis of the tests.

REFERENCES

1. D. Rawle, V. Rajagopal, C. G. Poncelet, R. J. Johnson and J. R. Himmelwright, "Spatial Stability Measurements on the Connecticut Yankee Reactor," Trans. Am. Nucl. Soc., 12, 766 (1969).
2. R. F. Barry, C. C. Emery, Jr., and T. D. Knight, "The PANDA Code," WCAP-7048 (April, 1967).
3. C. G. Poncelet, "Space Dependent Reactor Transfer Functions, Part I Theory," WCAP-2873 (March, 1966).
4. R. F. Barry, "The Revised LEOPARD Code - A Spectrum Dependent Non-Spatial Depletion Program," WCAP-2759 (March, 1965).
5. T. R. England, "CINDER - A One-Point Depletion and Fission Product Program" WAPD-TM-334 (August, 1962).
6. C. G. Poncelet and A. M. Christie, "Xenon-Induced Spatial Instabilities in Large Pressurized Water Reactors," WCAP-3680-20 (March, 1968).
7. C. G. Poncelet and A. M. Christie, "Time-Step Length Errors in Digital Simulation of Spatial Xenon Oscillations," Nuc. Sci. Eng., 42, 236 (1970).
8. R. H. Shudde and J. Dyer, "TEMPEST - A Neutron Thermalization Code," N.A.A. Deck 3W-354 (September, 1960).
9. M. K. Drake, Ed., "Data Formats and Procedure for the ENDF Neutron Cross Section Library," BNL-50274, ENDF-102, Vol. I (1970).